Published in final edited form as:
Science. 2013 February 22; 339(6122): 971–975. doi:10.1126/science.1229568.

Minimal "Self" Peptides That Inhibit Phagocytic Clearance and Enhance Delivery of Nanoparticles

Pia L. Rodriguez[1], **Takamasa Harada**[1], **David A. Christian**[1], **Diego A. Pantano**[1], **Richard K. Tsai**[1], and **Dennis E. Discher**[1,2,*]

[1]Molecular and Cell Biophysics and NanoBioPolymers Laboratory, University of Pennsylvania, Philadelphia, PA 19104, USA.

[2]Pharmacological Sciences Graduate Group, University of Pennsylvania, Philadelphia, PA 19104, USA.

Abstract

Foreign particles and cells are cleared from the body by phagocytes that must also recognize and avoid clearance of "self" cells. The membrane protein CD47 is reportedly a "marker of self" in mice that impedes phagocytosis of self by signaling through the phagocyte receptor CD172a. Minimal "Self" peptides were computationally designed from human CD47 and then synthesized and attached to virus-size particles for intravenous injection into mice that express a CD172a variant compatible with hCD47. Self peptides delay macrophage-mediated clearance of nanoparticles, which promotes persistent circulation that enhances dye and drug delivery to tumors. Self-peptide affinity for CD172a is near the optimum measured for human CD172a variants, and Self peptide also potently inhibits nanoparticle uptake mediated by the contractile cytoskeleton. The reductionist approach reveals the importance of human Self peptides and their utility in enhancing drug delivery and imaging.

Macrophages evolved to engulf and clear invading microbes and dying cells, but they respond similarly to injected particles, viruses, and implants, which hampers delivery of therapeutics and imaging agents. Coating of nanoparticles or liposomes with polyethylene glycol (PEG) creates "stealth" brushes that mimic a cell's glycocalyx and that delay immune clearance of foreign particles (1–3), but brushes can also hinder uptake by diseased cells (4). Neither a polymer brush nor a glycocalyx stops adsorption of abundant serum proteins, such as immunoglobulin G (IgG) (table S1), which promote clearance [e.g., (1–3, 5)], and any foreign polymer can also be immunogenic (6). Targeting diseased cells with ligand-modified particle constructs might make brushes unnecessary, but some ligands also promote rapid clearance by phagocytes (2, 7). In the reductionist approach here, we make a synthetic, human-based "Self" peptide that specifically binds and signals to phagocytes to inhibit clearance of particles as small as viruses.

*To whom correspondence should be addressed. discher@seas.upenn.edu.

P.L.R., D.A.P., and D.E.D. are authors on a patent applied for by the University of Pennsylvania on the Self peptide with first disclosure filed on 16 August 2010.

Supplementary Materials

www.sciencemag.org/cgi/content/full/339/6122/971/DC1

Materials and Methods
Figs. S1 to S10
Table S1
References (*32–44*)

CD47 glycoprotein is a putative “marker of self” in mice (8) and is expressed on all cell membranes in humans, mice, and other mammals (9). It associates in cis with integrins (10) and other species-specific, immunogenic complexes on cells (11–13). Mouse knockouts of CD47 (mCD47) are viable, but when red blood cells (mRBCs) from these mice are injected into the circulation of control mice, the deficient cells are cleared within hours by splenic macrophages, whereas normal mRBCs circulate for weeks (8). CD47’s extracellular domain interacts with CD172a (also known as signal regulatory protein-α, SIRPα) on phagocytes (10). Although binding is typically species-restricted (13), SIRPα is highly polymorphic, even within a species (14). Macrophages in nonobese diabetic/severe combined immunodeficient (NOD/SCID) strains of mice express a SIRPα variant that cross-reacts with human CD47 (hCD47), which explains why human hematopoietic cells engraft and circulate in NOD/SCID better than any other mice (14, 15). In vitro, the CD47-SIRPα interaction inhibits mouse macrophage uptake of antibody-coated mRBCs (8), as well as human macrophage uptake of both human RBCs (hRBCs) and hCD47-coated microparticles (16). This is not surprising as SIRPα signaling inhibits contractility-driven uptake of micron-size cells and particles (16). However, contractile forces are widely considered unimportant to internalization of nanoparticles and viruses, and so it is unclear whether this inhibitory interaction could be exploited in nanoparticle-based therapeutics.

We addressed whether hCD47 and a synthetic Self peptide can minimize phagocytic uptake of nanoparticles and thereby enhance delivery in NOD/SCID mice with X-linked severe combined immunodeficiency (*Il2rg*$^{-/-}$) mice (NSG). We first showed that blocking mCD47 accelerates clearance of mRBCs in NSG mice. Cells (or nanobeads) were split into two samples, with one sample labeled by red fluorophore and the other sample labeled by far-red fluorophore plus antibody against mCD47. The samples were mixed 1:1 for injection into the same mouse, and blood samples at subsequent time points were analyzed by flow cytometry for both colors, which produced a ratio (fig. S1A) that minimizes mouse-to-mouse variations. IgG and other serum proteins physisorb in vivo to RBCs (17), viruses (18), and PEGylated nanoparticles (19) (table S1), but in NSG mice, IgG is very low or not detectable (versus ~100 μM in normal animals). Controlled opsonization with IgG was therefore used in most of our studies to better mimic immune-competent animals. With RBCs, mRBC-specific antibody was added to promote clearance via phagocytosis (20). Consistent with a marker-of-self function of mCD47, the persistence ratio for the mixed sample [mRBCs/(mRBCs with blocked mCD47)] increased exponentially with a doubling time (*T*) of 33 min (Fig. 1B); single-color analyses also give *T* = 30 min (fig. S1B).

RBC membranes have hundreds of different interacting proteins, and many involved in clearance are different for mouse and humans (12, 21). To give a better-defined surface for reductionist studies in vivo and also to begin testing the marker-of-Self concept on foreign particles of potential use for imaging and therapy, the extracellular immunoglobulin-like domain of hCD47, which binds SIRPα, was recombinantly expressed; site-specifically biotinylated; and then bound to streptavidin-coated, 160-nm polystyrene nanobeads. Beads were also labeled with red or near-infrared dyes (or left unlabeled) and controllably opsonized with either antibody against streptavidin (fig. S1C) or a biotinylated antibody for targeting (fig. S1D). After injection into an NSG mouse, blood analysis by flow cytometry clearly identified nanobeads on the basis of both distinctive scatter and fluorescence detection of the opsonizing antibody ± hCD47 (Fig. 1A and fig. S1, A and C). A persistence ratio for [(nanobead + hCD47)/nanobead] was well-controlled at every time point and again increased exponentially with a doubling time (*T*) of 33 ± 8 min (Fig. 1C). Mice injected with a single color of nanobead gave similar results (*T* = 31 min) (fig. S1E). PEG-biotin nanobeads that were also preopsonized showed a flat persistence curve (*T* > 200 min), consistent with the fact that PEG brushes alone do not directly inhibit clearance by macrophages (fig. S2, A to C). In the absence of preopsonization, PEG-nanobeads did

circulate for hours as expected, but hCD47, once again, enhanced circulation (fig. S2D). hCD47 on virus-size particles is thus an inhibitor of in vivo clearance and thereby prolongs circulation.

Minimization of the 117–amino acid immunoglobulin-like domain of hCD47 to a small, binding-site Self peptide could provide key evidence that signaling to mouse SIRPα (mSIRPα) is part of the molecular mechanism for inhibiting clearance in vivo. A crystal structure of hCD47-hSIRPα suggests three distinct binding sites (22), but the highest density of interactions are in one loop in hCD47 between canonical β strands F and G, where a nine–amino acid sequence constitutes 40% of hCD47's contacting residues (Fig. 1A, structure). We designed by simulation a 21–amino acid Self peptide around this sequence with the aims of minimizing species specificity (13) and eliminating glycosylation of CD47, which impedes binding (23). Biotinylation on an amino-terminal PEG linker provided a means of attachment to streptavidin beads for in vivo studies. Relative to control nanobeads, the Self peptide increased the persistence of beads in the circulation with a mean doubling time, *T*, of 20 ± 3 min, whereas Scrambled peptide (see supplementary materials) had little impact on circulation (Fig. 1C). An apparent difference in persistence in the circulation between Self peptide and hCD47 is not significant ($P = 0.18$).

Prolonged circulation of hCD47 beads and Self beads is based on a delay of phagocytic clearance by the spleen and perhaps liver, but nanobeads localize nonetheless to these organs in whole-body imaging of near-infrared fluorescent (NIRF) beads (Fig. 2A and fig. S3, A to D) by interactions that are likely similar to those that promote RBC adhesion in spleen and greatly increase splenic hematocrit (24). Recombinant mCD47 also enhanced persistence in circulation and again showed moderate but suppressed splenic localization (fig. S3B). For additional insight into persistent circulation and potential therapeutic application of Self-nanoparticles, human-derived A549 lung adenocarcinoma epithelial cells were grafted into the flanks of NSG mice, NIRF nanobeads were injected into the tail veins weeks later, and the tumors were imaged both in vivo and ex vivo to quantify accumulated signal. As early as 10 min post injection, hCD47 and Self nanobeads gave mean tumor intensities twice those of noninjected mice, whereas control beads gave background-level signal (Fig. 2B).With hCD47 and Self nanobeads, the fluorescence at every time point is statistically similar but significantly higher than that of control beads ($P < 0.05$), and the increase fits first-order kinetics ($\tau = 52$ min), consistent with enhanced perfusion and progressive clearance. At 40 min, both hCD47 and Self nanobeads give higher signals than controls, ~10 to 20 times as much, and a second injection of hCD47 nanobeads after 2 hours showed a similar signal increase (fig. S4, A and B). Tumor accumulation fits a first-order process (with $\tau = 52$ min giving $T = \tau \ln 2 = 36$ min) that is much faster than control beads ($T = 210$ min), and both time scales are similar to those obtained for persistent circulation (Fig. 1C), consistent with the hypothesis that enhanced tumor signal results from persistent circulation.

After in situ imaging, tumors and other major organs were subsequently excised and imaged ex vivo (fig. S4C). The Self beads and hCD47 beads show at least 16- to 22-fold enhancement of the very low signals obtained with control beads either with or without Scrambled peptide, with no statistical difference between Self peptide and hCD47. The fraction of nanobeads in the blood within the tumor is small (fig. S4C, inset), and so the majority of signal derives from beads that have accumulated in the tumor, most likely by enhanced permeation and retention (EPR) through the leaky vasculature that is characteristic of many solid tumors (25). On the basis of these results, the hydrophobic anticancer drug paclitaxel (Tax) was loaded into the Self nanobeads, as well as into beads with PEG and/or antibody against hCD47 (fig. S5, A and B). The latter antibodies have been used therapeutically to mask self on cancer cells (26), but targeting antibodies are a double-edged

sword when attached to beads, because they also promote clearance (fig. S1D). Tax-loaded beads that displayed either recombinant hCD47 (fig. S5C) or Self-peptide plus PEG and hCD47-targeting antibody (fig. S5D) consistently shrank tumors more than beads lacking Self. The Self beads also did as well or better than the standard paclitaxel nanocarrier Cremophore, which is known for its toxic side effects (e.g., fig. S5, E and F). The NSG mouse results thus reveal active suppression of clearance by both hCD47 and Self peptide, which could enhance both tumor imaging and drug delivery.

Flow cytometry enables detailed analysis of the surface of nanobeads sampled from circulation. Although streptavidin-specific IgG remains stably bound, biotinylated hCD47 is partially lost (30% in Fig. 3A, inset bar graph; fig. S6A). Nonetheless, the percentage clearance of nanobeads at 35 min versus the measured density of hCD47 at 35 min fits an inhibition model (Fig. 3A) with the inhibition constant $K_{i,\ in\text{-}vivo}$ of 110 molecules per 160-nm nanobead. This appears independent of circulating bead number over at least a ~10-fold range (fig. S6B). This $K_{i,in\text{-}vivo}$ corresponds to a density of hCD47 that is 10 times that of the lowest densities reported for hRBCs [~25 hCD47 molecules/μm^2 (12)] but ~1/100th of nanobead saturation (e.g., fig. S2A). Although binding of soluble hCD47 to NSG-SIRPα$^+$ phagocytes yields a weak affinity (K_d = 4 μM) (Fig. 3B), lymphocytes, which do not express SIRPα (27), show zero binding. In vivo evidence of interaction specificity was also obtained by preinjecting mSIRPα-specific antibody, which blocks hCD47 binding, followed by injection of Self nanobeads; these beads were cleared as if lacking Self (Fig. 3B, inset).

To compare the effective affinity of NSG mouse to human SIRPα (hSIRPα), 10 human polymorphic variants of hSIRPα (14) were expressed on Chinese hamster ovary (CHO) cell membranes (24). Saturation binding of soluble hCD47 to each variant yielded a 60-fold range of affinities with K_d = 0.08 to 5 μM (Fig. 3C and fig. S7), even though all of the amino acid differences in the variants are outside of the binding interface (22). When plotted against the allele frequency of hSIRPα, variants of intermediate affinity (e.g., v1 and v2) are most common, with affinities similar to that for soluble SIRPα(v1) binding to CHO-displayed hCD47 (23). hCD47's affinity for NSG-SIRPα phagocytes is within the range of reported hSIRPα variants and so is the affinity of Self peptide for the most common SIRPα variant. Synthesis and simulations of additional peptides (Fig. 3D and fig. S8) reveal a sensitivity of binding to conformation, as well as sequence, and show that a lack of affinity for hSIRPα is predictive of a failure to inhibit in vitro phagocytosis.

Whether phagocytosis of nanoparticles—including viruses—involves mechanisms similar to those for larger particles remains an open question (28). Tissue sections show that nanobeads colocalize with macrophages (Fig. 4A, *i*). In cultures of human-derived monocytic cell line THP1 macrophages, nanoparticles are not dense enough to settle and contact cells, but opsonized nanobeads that are added at the same total surface area as microbeads (fig. S9A) are taken up with equal efficiency (Fig. 4A, *ii*, *a*). Myosin-II accumulates at the phagocytic synapse formed with opsonized beads except when hCD47 is attached (Fig. 4A, *ii*, *a* and *b*). Microparticles and microbes (i.e., bacteria) give similar images (fig. S9B), and inhibition of phagocytic uptake by hCD47 is indeed independent of particle size from at least 100 nm to 10 μm (Fig. 4A, *ii*, *c*; and fig. S9C). Similar inhibition of nanobead uptake was found with biotinylated Self peptides, whereas both Scrambled peptide and disulfide-bridged peptide (Self-SS) showed no significant inhibition of uptake (Fig. 3D, *i* and *ii*). The potency of hCD47 is remarkable with $K_{i,in\text{-}vitro} \approx 1.0 \pm 0.3$ molecule per 45,000 nm^2. Equivalently, a nanoparticle of 60-nm radius requires only one CD47 molecule to inhibit uptake. $K_{i,in\text{-}vitro}$ is the same as the lowest densities reported for hRBCs (12) and is far smaller than PEG densities needed to enhance nanoparticle circulation through delayed opsonization (e.g., fig. S2A: >1 PEG per 20 nm^2).

IgG-driven uptake is linear in myosin-II activity (16). With the nanobeads described here, both drug inhibition of myosin-II and hCD47 inhibit uptake by up to 80% (Fig. 4A, *ii*, *c*). When CD47 binds SIRPα, SIRPα's cytoplasmic tail is hyperphosphorylated to activate SHP1 phosphatase (29), which dephosphorylates multiple proteins, including myosin-II (16). Inhibition of SHP1 produces the expected increase in phagocytosis of hCD47 beads (Fig. 4A, *ii*, *c*; and fig. S9D), and binding of hCD47 and Self peptide indeed increases phospho-SIRPα (Fig. 4B). Consistent with a common mechanism in vitro and in vivo, uptake of the various nanoparticles by THP1 cells correlates inversely with persistence in NSG mice (Fig. 4C).

Phagocytes pervade all tissues and disease sites, with key roles in recognition and clearance, as well as contributions to pro- and anti-inflammatory responses with cytokine release and oxidative burst. Whether synthetic Self peptides, CD47, or its homologs are displayed on particles, viruses (30), or artificial surfaces (31), "active stealth" signaling across length scales (fig. S10) offers additional opportunities in application as well as understanding. In particular, the SIRPα polymorphism results suggest that an intermediate affinity for Self is optimal (Fig. 3C) as a trade-off between adhesion that is not too strong ("must let go") and signaling that is not too weak ("don't eat me"). Additional homeostatic self factors seem likely and might similarly be used to further avoid phagocytes and thereby enhance delivery of therapeutics and imaging agents.

Supplementary Material

Refer to Web version on PubMed Central for supplementary material.

Acknowledgments

The assistance of A. Secreto, J. Glover, and G. Danet-Desnoyers of the Stem Cell Xenograft Core at the University of Pennsylvania is very gratefully acknowledged as is technical assistance of K. Hsu, P. Bhoorasingh, and V. Carnevale. Support from the NIH (R01-EB007049, R01-HL062352, P01-DK032094, NCATS-8UL1TR000003, P30-DK090969) and NSF (Materials Research Science and Engineering Center, and Nano Science and Engineering Center-Nano Bio Interface Center) is also very gratefully acknowledged.

References and Notes

1. Bartlett DW, Su H, Hildebrandt IJ, Weber WA, Davis ME. Proc. Natl. Acad. Sci. U.S.A. 2007; 104:15549. [PubMed: 17875985]
2. Klibanov AL, Maruyama K, Beckerleg AM, Torchilin VP, Huang L. Biochim. Biophys. Acta. 1991; 1062:142. [PubMed: 2004104]
3. Photos PJ, Bacakova L, Discher B, Bates FS, Discher DE. J. Control. Release. 2003; 90:323. [PubMed: 12880699]
4. Hong RL, et al. Clin. Cancer Res. 1999; 5:3645. [PubMed: 10589782]
5. Rossin R, Muro S, Welch MJ, Muzykantov VR, Schuster DP. J. Nucl. Med. 2008; 49:103. [PubMed: 18077519]
6. Armstrong JK, et al. Cancer. 2007; 110:103. [PubMed: 17516438]
7. Turk MJ, Waters DJ, Low PS. Cancer Lett. 2004; 213:165. [PubMed: 15327831]
8. Oldenborg PA, et al. Science. 2000; 288:2051. [PubMed: 10856220]
9. Bentley AA, Adams JC. Mol. Biol. Evol. 2010; 27:2187. [PubMed: 20427418]
10. Brown EJ, Frazier WA. Trends Cell Biol. 2001; 11:130. [PubMed: 11306274]
11. Bruce LJ, et al. Blood. 2003; 101:4180. [PubMed: 12531814]
12. Mouro-Chanteloup I, et al. Blood. 2003; 101:338. [PubMed: 12393467]
13. Subramanian S, Parthasarathy R, Sen S, Boder ET, Discher DE. Blood. 2006; 107:2548. [PubMed: 16291597]

14. Takenaka K, et al. Nat. Immunol. 2007; 8:1313. [PubMed: 17982459]
15. Strowig T, et al. Proc. Natl. Acad. Sci. U.S.A. 2011; 108:13218. [PubMed: 21788509]
16. Tsai RK, Discher DE. J. Cell Biol. 2008; 180:989. [PubMed: 18332220]
17. Turrini F, Mannu F, Arese P, Yuan J, Low PS. Blood. 1993; 81:3146. [PubMed: 8499648]
18. Wilflingseder D, et al. J. Immunol. 2007; 178:7840. [PubMed: 17548622]
19. Lundqvist M, et al. Proc. Natl. Acad. Sci. U.S.A. 2008; 105:14265. [PubMed: 18809927]
20. Cox D, Greenberg S. Semin. Immunol. 2001; 13:339. [PubMed: 11708889]
21. Glodek AM, et al. Blood. 2010; 116:6063. [PubMed: 20861458]
22. Hatherley D, et al. Mol. Cell. 2008; 31:266. [PubMed: 18657508]
23. Subramanian S, Boder ET, Discher DE. J. Biol. Chem. 2007; 282:1805. [PubMed: 17098740]
24. MacDonald IC, Schmidt EE, Groom AC. Microvasc. Res. 1991; 42:60. [PubMed: 1921755]
25. Matsumura Y, Maeda H. Cancer Res. 1986; 46:6387. [PubMed: 2946403]
26. Willingham SB, et al. Proc. Natl. Acad. Sci. U.S.A. 2012; 109:6662. [PubMed: 22451913]
27. Seiffert M, et al. Blood. 1999; 94:3633. [PubMed: 10572074]
28. Swanson JA, Hoppe AD. J. Leukoc. Biol. 2004; 76:1093. [PubMed: 15466916]
29. Matozaki T, Murata Y, Okazawa H, Ohnishi H. Trends Cell Biol. 2009; 19:72. [PubMed: 19144521]
30. Cameron CM, Barrett JW, Mann M, Lucas A, McFadden G. Virology. 2005; 337:55. [PubMed: 15914220]
31. Stachelek SJ, et al. Biomaterials. 2011; 32:4317. [PubMed: 21429575]

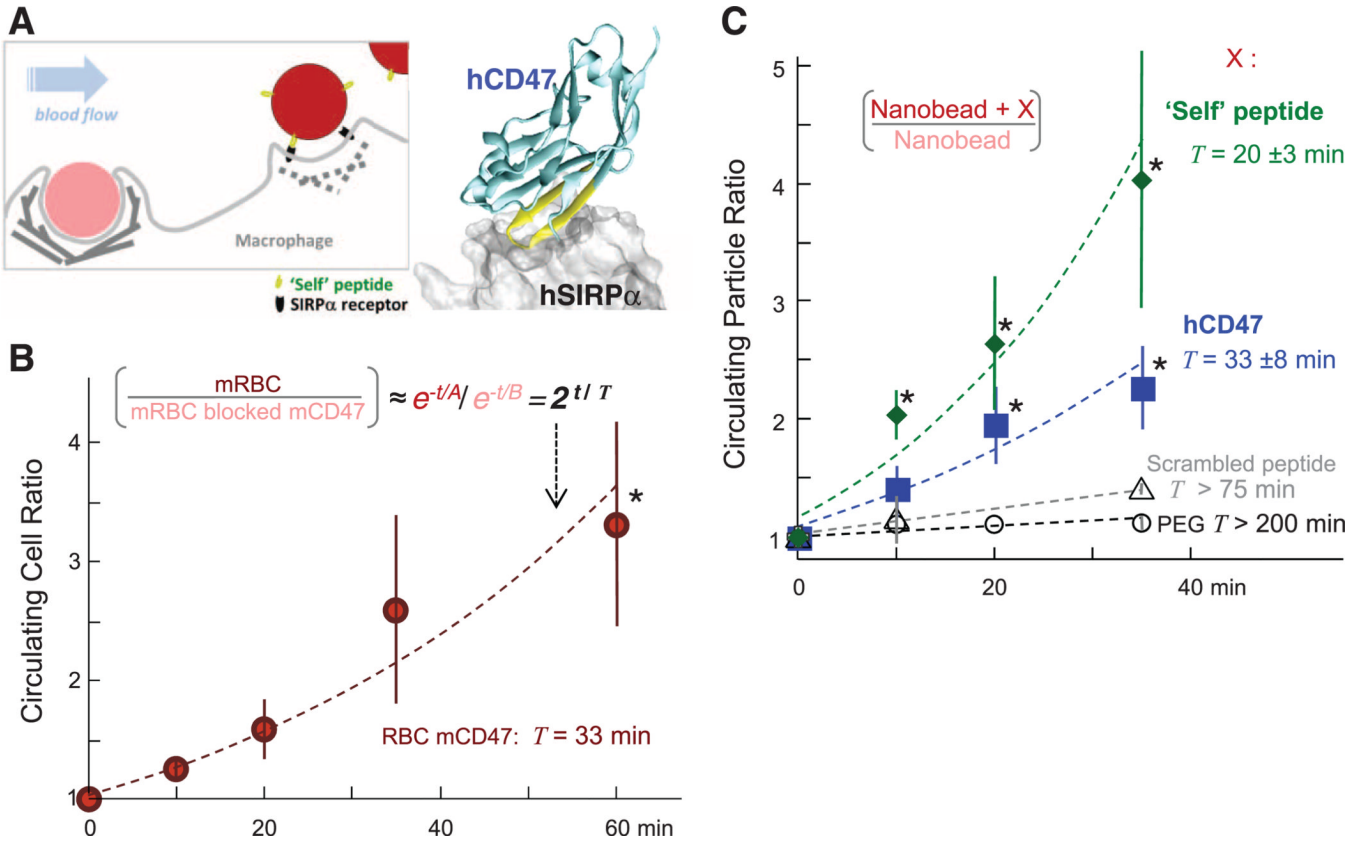

Fig. 1. Self peptide and hCD47 prolong the circulation of nanobeads in NSG mice

(**A**) Competitive circulation in which two colors of nanobeads or cells injected into the same mouse are flowing with blood and being cleared by a splenic macrophage (left) or else recognized as self and released (right). Blood was sampled periodically in the experiment (50 μl), and flow cytometry analysis yields the bead or cell ratio in each mouse at each time point. The cocrystal structure shows hCD47 with the Self peptide binding hSIRPα. (**B**) Competitive circulation experiment in which mRBCs from NSG mice were either blocked with anti-CD47 or not and were also opsonized with excess mRBC-specific antibody before cells were mixed together and injected into the tail vein. Both color cell types are cleared with clearance constants ~*A* or *B* (*A* > *B*), and the ratio of exponentials gives the persistence ratio doubling time *T* (*n* = 3 mice; R^2 = 0.93 for fit of means with indicated *T*). (**C**) Circulation experiments used 160-nm polystyrene beads with covalently attached streptavidin incubated with biotinylated versions of one of the following: synthetic Self peptide (*n* = 4; R^2 = 0.94 for fit of means); recombinant hCD47 (*n* = 6; R^2 = 0.92 for fit of means); or negative controls of either Scrambled peptide (*n* = 3) or PEG (*n* = 5). Nanobeads were also opsonized with streptavidin-specific antibody, and then 10^7 were injected. Flow cytometry quantification was typically done on 100 to 10,000 particles at each time point and typically included quantification of both hCD47 and opsonin on the nanobeads. For hCD47 and Self peptide, a separate fit for each mouse gives the indicated mean *T* ± SEM for each group, which is within 10% of the *T* obtained from fitting the group averages (dashed curves). Most data points for hCD47 and Self peptide differ significantly from PEG-nanobeads (*P < 0.05). All data are means ± SEM.

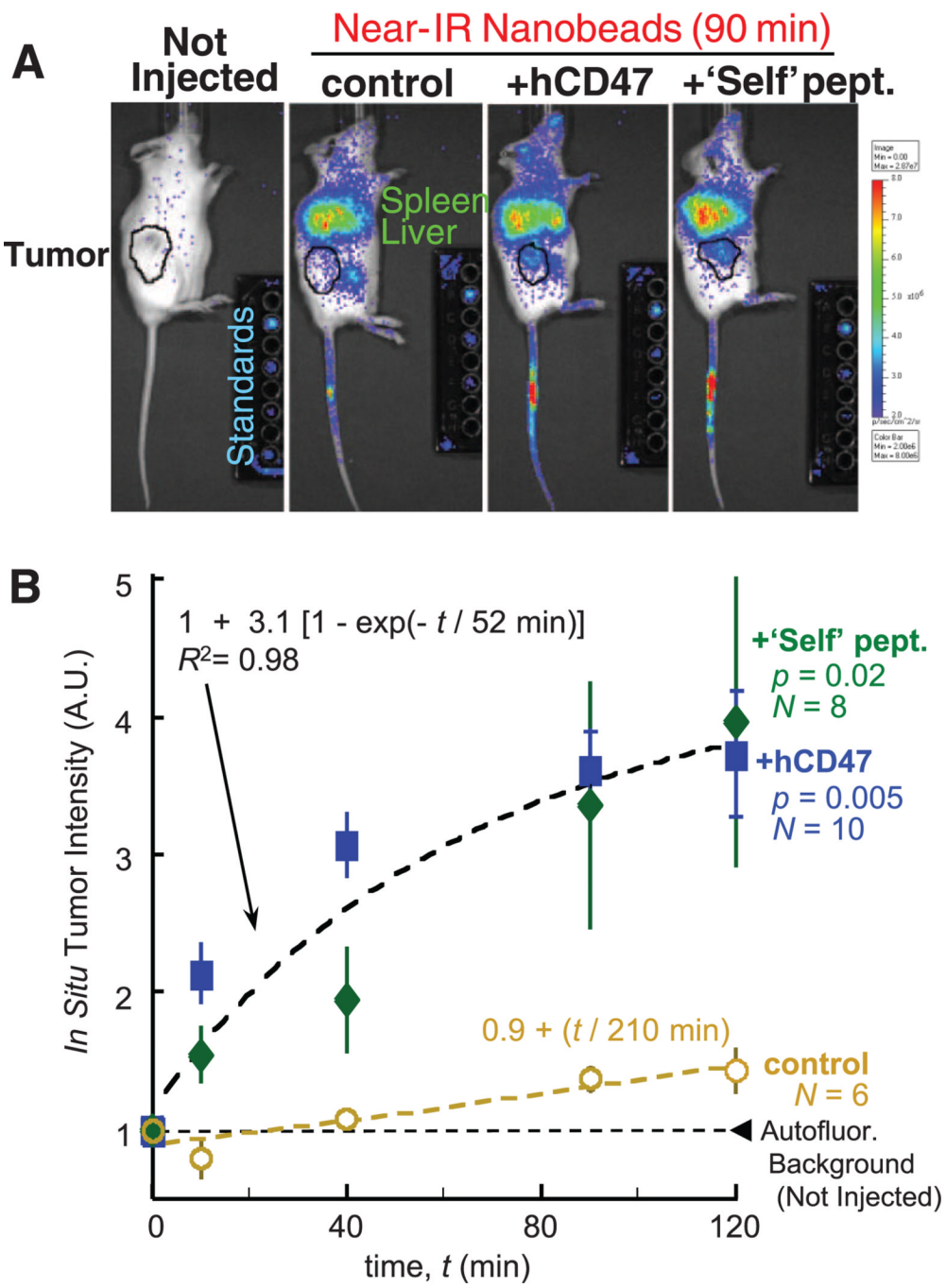

Fig. 2. Self peptide and hCD47 enhance tumor imaging by near-infrared particles

(**A**) NSG mice with flank tumors of A549 lung–derived cells (black circles) received tail vein injections of nanobead mixtures in which one bead type is labeled with DiR fluorophore. Images of live mice and calibration standards were taken with a Xenogen imager. Tumor-bearing mice have persistence ratios of particles in blood at 35 min, similar to results in Fig. 1C, even though many particles are seen in spleen and liver. (**B**) The tumor was located by bright-field imaging, and total fluorescence was quantified at each time point. All results for Self peptide and hCD47 were combined in the fit. *N*, Number of tumors from three different sets of tumor-bearing mice. All data are means ± SEM.

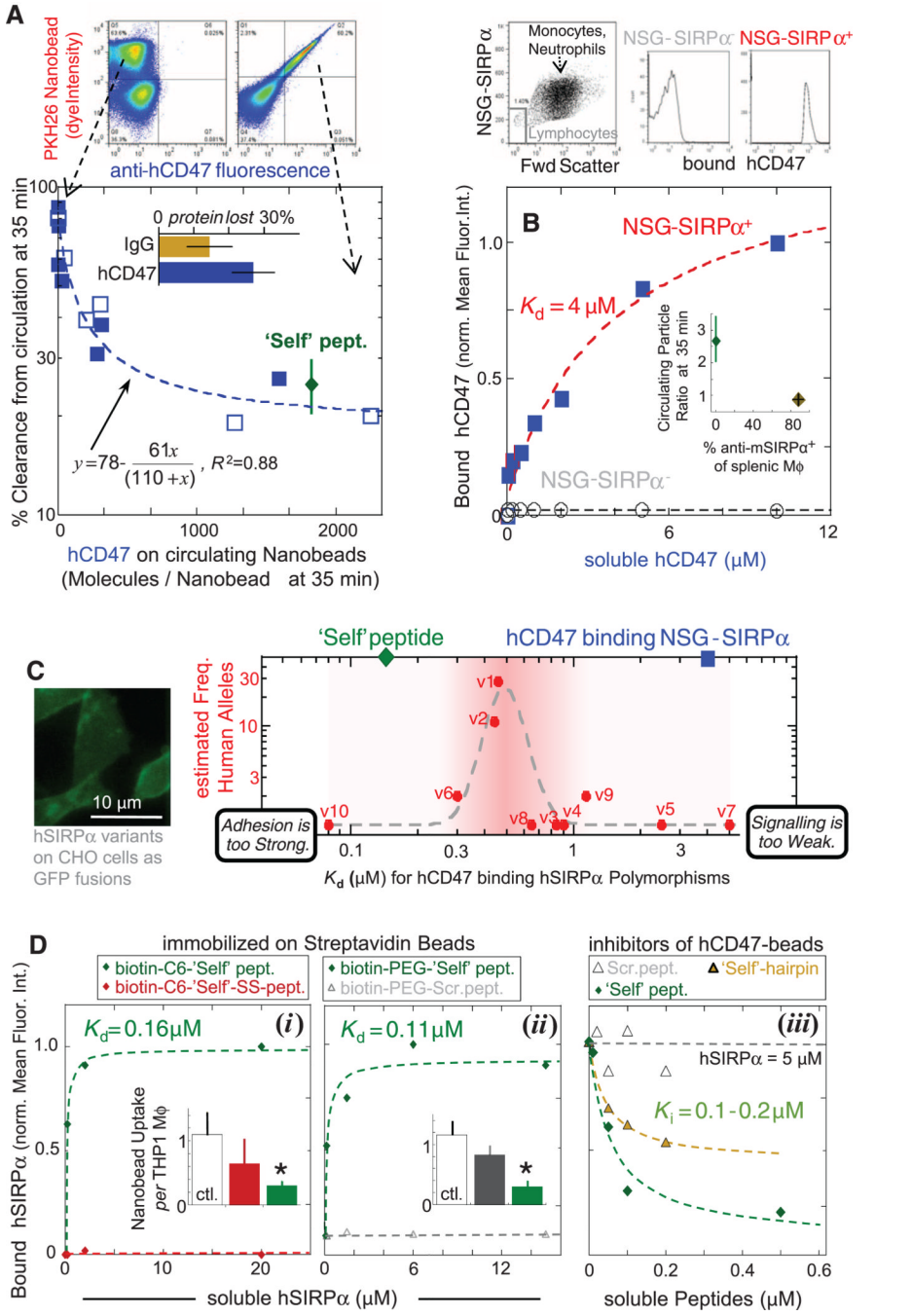

Fig. 3. Persistence of hCD47 and Self nanobeads depends on hCD47 density, consistent with low-affinity binding to NSG mSIRPα relative to hSIRPα variants

(**A**) The number of hCD47 molecules on the 160-nm beads 35 min after injection was either measured in two-color experiments (solid symbols; n = 7 mice) or single-color experiments (open symbols; n = 6 mice), with an average of 30% protein lost in circulation (inset). Self peptide levels are estimated to have a similar loss (n = 4 mice). Fluorescent nanobeads ($PKH26^+$ in flow cytometry, top) were confirmed by forward and/or side scatter, and fluorescent hCD47-specific antibody measured hCD47 levels (left, control nanobead sample; right, hCD47 nanobead sample). The inhibition curve gives K_i = 110 molecules/nanobead. (**B**) Affinity of soluble hCD47 for NSG neutrophils and monocytes, from flow

cytometry analysis of Cy5-biotin–specific antibody. Lymphocytes are negative for SIRPα and do not bind soluble hCD47. (Inset) Preinjection of blocking anti-mSIRPα eliminates the enhanced circulation of Self nanobeads of Fig. 1C. After 35 min, most splenic macrophages (Mφ: F4/80 antibody+) have mSIRPα antibody on their surface (n = 4 mice). (**C**) Ten reported variants of hSIRPα's N-terminal domain (14) were displayed on CHO cells to determine effective K_d values for soluble hCD47; soluble hSIRPα binding to hCD47 beads showed the same trend (fig. S7E). The putative allele frequency (14) is highest at intermediate K_d, whereas the affinity of hCD47 for mSIRPα on NSG phagocytes (blue square) is weaker and that of Self peptide for hSIRPα(v1) is stronger (green diamond). The Lorentzian fit is inspired by other mechanobiological signaling processes and has the form: $y = 1 + 0.05x^{11}/(0.50^{11} + x^{11})^2$, $R^2 = 0.85$. (**D**) Binding of peptides on beads to soluble hSIRPα (v1) was assayed by flow cytometry. Neither the Self-SS peptide with a T107C substitution nor the Scrambled peptide bind hSIRPα. The assays in (*iii*) use soluble peptides and show the 10–amino acid Self hairpin centered on the loop is a partial inhibitor. Bar graph insets in (*i* and *ii*) show in vitro phagocytosis assay results with the human THP1 cell line, which demonstrates that only the Self peptide (attached to biotin via either PEG or C6, 6-aminohexanoic acid) significantly inhibits phagocytic uptake (*P < 0.05 different from control). All data are means ± SEM.

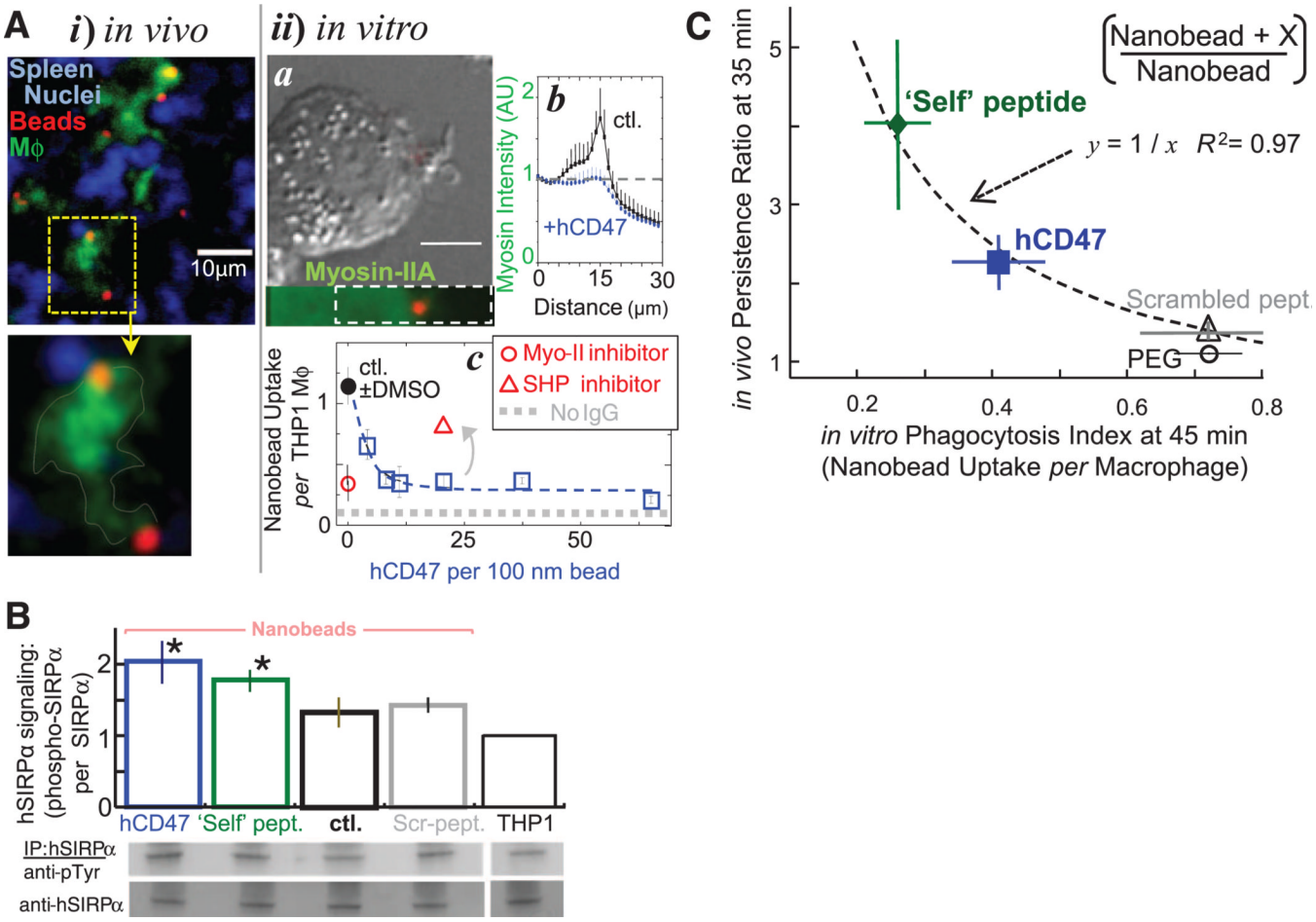

Fig. 4. Phagocytosis of nanobeads is efficient and recruits myosin-II, unless CD47 or Self peptide bind SIRPα and signal inhibition through SHP1

(**A**) Nanobead uptake in NSG mice and in vitro with human-derived THP1 macrophages. (*i*) Splenic macrophages colocalize with nanoparticles in situ. Spleens harvested after 35 to 40 min were frozen, sectioned, fixed, and permeabilized for immunostaining green for macrophages (Mφ) and red with a secondary antibody against streptavidin-coated opsonized beads [goat antirabbit F(ab′)$_2$]. Nuclei are stained blue with Hoechst dye. (*ii*) Phagocytosis of fluorescent 100-nm beads (red) by THP1 cells in vitro was assessed at 45 min by immunostaining cultures that were fixed (but not cell permeabilized) for noningested beads by using secondary antibody against antistreptavidin. Nonmuscle myosin-IIA (*a*, bottom) enriches near the nanoparticle unless hCD47 is on the bead (*b*, plot). Enrichment extends deeply into the cytoplasm (~5 μm) relative to bead size, suggestive of a diffuse signal that directs cytoskeletal assembly. Nanobeads with antistreptavidin are readily engulfed at about 1 bead per cell (*c*), but uptake is inhibited by hCD47 and by inhibition of myosin-IIA with blebbistatin (50 μM). Inhibition of SHP1, downstream of SIRPα, with NSC-87877 blocks the inhibition of uptake by hCD47. Dimethyl sulfoxide (DMSO) is the solvent for the drugs. (**B**) Phosphorylation of hSIRPα tyrosines in THP1 cells upon contact with opsonized nanobeads bearing hCD47 and Self peptide. hSIRPα was immunoprecipitated from cell lysates, and phosphotyrosine was immunoblotted for quantification ($n = 3$; $^*P < 0.05$). (**C**) Inverse correlation between in vivo persistence ratio at 35 min and in vitro inhibition of phagocytosis by hCD47 and Self peptide at 45 min for 160-nm beads. All data are means ± SEM.